Data Files (Appendix 1): 宮田和周・中田健太郎・柴田正輝・長田充弘・永野裕二・大藤　茂・中山健太朗・安里開士・中谷大輔・小平将大, 2023, 長崎半島東岸長崎市北浦町の上部白亜系層序の再定義とその地質年代学的意義. 地質雑, **129** [Miyata, K., Nakada, K., Shibata, M., Nagata, M., Nagano, Y., Otoh, S., Nakayama, K., Asato, K., Nakatani, D. and Kodaira, S., 2023, Redefining of the Upper Cretaceous stratigraphy on the eastern coast of the Nagasaki Peninsula (Kitaura, Nagasaki City), northwestern Kyushu, Japan, and its geochronological significance. *J. Geol. Soc. Japan*, **129**]

Appendix 1. Zircon separation, U–Pb dating method, and results.

Zircon separation, U–Pb dating method, and results

by M. Nagata, Y. Nagano and S. Otoh

1. Sample

We collected sandstone sample ASMM from the sandstone-rich exposure of the Akasakino-hana Sandstone and Mudstone Member of the Nagasaki Kitaura Formation that was closest to the fault with the underlying Nomozaki Formation (32° 42′ 22.6″ N, 129° 55′ 16.7″ E; see also Fig. 3). The sandstone consists mainly of quartz, plagioclase, alkali feldspar, chlorite, and epidote.

2. Zircon separation and U–Pb dating

The procedures of zircon separation are the same as those of Nagata et al. (2020) and Nagata and Otoh (2020, 2021). The zircons were hand-picked from the residue after crushing, water elutriation, panning, and separation of magnetic and low-density minerals and then were embedded in resin. Cathodoluminescence (CL) images of the zircons were taken on a scanning electron microscope (JEOL JSM-6610 LV) with a Gatan Mini CL equipped in the Geological Survey of Japan (GSJ), the National Institute of Advanced Industrial Science and Technology, Japan (AIST). The age-dating of the zircons was carried out using the laser ablation-inductively coupled plasma mass spectrometer (LA-ICPMS) at the Graduate School of Environmental Studies, Nagoya University. The laser ablation system was UP-213 of New Wave Research, inc., and the ICPMS was Agilent 7700x of Agilent Technologies. We used the NIST SRM 610 glass (Horn and von Blankenburg, 2007) normalized by 91500 zircon (Wiedenbeck et al., 1995) for elemental- and isotopic-ratio corrections. 91500 and OD-3 (Iwano et al., 2013) zircons were measured together with unknown samples to confirm the effectiveness of the corrections. Details of the analytical conditions are in Table A1 (see also Kouchi et al., 2015), and details of the zircon U–Pb isotopic data are in Tables A2 and A3. The $^{207}Pb/^{206}Pb$ ages are noted only for the data set where the $^{207}Pb/^{235}U$ and $^{206}Pb/^{238}U$ ages are both 1000 Ma or older. We adopted only the data with the error ellipse overlapping with the concordia curves of the normal concordia plot, drawn from the $^{207}Pb/^{206}Pb$, $^{207}Pb/^{235}U$, and $^{206}Pb/^{238}U$ ratios and their errors (2SD; standard deviation) using Isoplot 4.15 (Ludwig, 2012). We use the $^{206}Pb/^{238}U$ age of adopted data sets in the following description. The weighted average of the $^{206}Pb/^{238}U$ age for the 91500 and OD-3 zircons measured with the zircons from sample ASMM were 1062.6 ± 7.1 Ma and 32.86 ± 0.56 Ma, respectively (Tables A1, A2). These values include their recommended ages (Wiedenbeck et al., 1995; Iwano et al., 2013) within their error ranges, respectively.

3. Measurement results

A total of 104 zircons from sample ASMM were measured (Fig. A1a; Table A3). Among them, 81 adopted ages were of Cretaceous (ca. 132–84 Ma, 74 grains: 91.4%), Jurassic (ca. 182–173 Ma, 4 grains: 5.0%), Triassic (ca. 182–173 Ma, 1 grain: 1.2%), Permian (ca. 182–173 Ma, 1 grain: 1.2%), and Neoproterozoic (ca. 891 Ma, 1 grain: 1.2%; Fig. A1b), with Th/U values ranging from 0.30 to 2.16 (Table A3). The Cretaceous zircons made two peaks, ca. 132–94 Ma and ca. 87–84 Ma, on the probability density plot (Fig. A1c). The youngest data in the ca. 87–84 Ma age cluster, which made up of 12 data, was 83.6 ± 5.0 Ma, with the error range overlapping with that of the other 11 data. We obtained the weighted mean $^{206}Pb/^{238}U$ age of 85.74 ± 0.75 Ma (95% confidence, MSWD = 0.59, Probability = 0.83) from this age cluster (Fig. A1d).

4. References

Gale, N. H. and Mussett, A. E., 1973, Episodic uranium–lead models and the interpretation of variations in the isotopic composition of lead in rocks. *Reviews of Geophysics*, **11**, 37–86.

Horn, I. and Blanckenburg, F. V., 2007, Investigation on elemental and isotopic fractionation during 196 nm femtosecond laser ablation multiple collector inductively coupled plasma mass spectrometry. *Spectrochim. Acta*, *Part B*, **62**, 410–422.

Iwano, H., Orihashi, Y., Hirata, T., Ogasawara, M., Danhara, T., Horie, K.,...Yamamoto, K., 2013, An inter-laboratory evaluation of OD-3 zircon for use as a secondary U–Pb dating standard. *Isl. Arc*, **22**, 382–394.

Kouchi, Y., Orihashi, Y., Obara, H., Fujimoto, T., Haruta, Y. and Yamamoto, K., 2015, Zircon U–Pb dating by 213 nm Nd: YAG laser ablation inductively coupled plasma mass spectrometry: Optimization of the analytical condition to use NIST SRM 610 for Pb/U fractionation correction. *Geochemistry* (*Chikyukagaku*), **49**, 19–35.*

Ludwig, K. R., 2012, *User's Manual for Isoplot 3.75–4.15: Geochronological Toolkit for Microsoft Excel*. Berkeley Geochronology Center Special Publication 5, 77p.

Nagata, M., Kouchi, Y. and Otoh, S., 2020, Early Cretaceous U–Pb dates of zircons from the Kabashima Granite in the Nomo Peninsula, Nagasaki Prefecture, SW Japan. *J. Geol. Soc. Japan*, **126**, 333–339.*

Nagata, M. and Otoh, S., 2020, New U–Pb zircon dates from the Pankehoronai Unit of the Kamuikotan metamorphic rocks in central Hokkaido. *J. Geol. Soc. Japan*, **126**, 597–601.*

Nagata, M. and Otoh, S., 2021, The U–Pb zircon dates from the Maeshima Granodiorite in Amakusa City, Kumamoto Prefecture, Southwest Japan. *J. Geol. Soc. Japan*, **127**, 237–243.*

Wiedenbeck, M., Alle, P., Corfu, F., Griffin, W. L., Meier, M., Oberli, F., …Spiegel, W., 1995, Three natural zircon standards for U–Th–Pb, Lu–Hf, trace element and REE analyses. *Geostand. Newsl.*, **19**, 1–23.

* in Japanese with English abstract

5. Table, figure and captions

Table A1. LA-ICPMS anlaytical settings and conditions for the U–Pb zircon dating.

Laser Ablation System			
Instrument	NWR-213 frequency quadrupled Nd-YAG laser		
Laser wave length	213 nm		
Repetition rate	10 Hz		
Spot size	25 µm		
Ablation time	8 s (Pre-ablation) + 10 s		
He gas flow rate	1.0 L / min		
Inductively Coupled Plasma Mass Spectrometer			
Instrument	Agilent 7700x		
Forward power	1400 W		
Monitor elements	^{202}Hg, ^{204}(Hg + Pb), ^{206}Pb, ^{207}Pb, ^{208}Pb, ^{232}Th, ^{238}U		
Ar gas flow rate	0.9–1.1 L / min		
Scan mode	Peak jumping mode		
Detecer mode	Pulse counting		
Standard Materials			
Primary standard	**NIST SRM 610 glass nomarized by 91500 zircon**		
%2SD	^{206}Pb/^{238}U	^{207}Pb/^{206}Pb	^{208}Pb/^{232}Th
	1.1–3.0	1.0–4.6	1.2–2.4
Secondary standard	**91500 zircon** ^{207}Pb/^{206}Pb weighted mean: 1074 ± 20 Ma (N = 13; 95% confidence) ^{206}Pb/^{238}U weighted mean: 1062.6 ± 7.1 Ma (N =13; 95% confidence) **OD-3 zircon** ^{206}Pb/^{238}U weighted mean: 32.86 ± 0.56 Ma (N = 12/13; 95% confidence)		
Data Processing			
Normalization value	^{206}Pb/^{238}U: 0.2236 (Horn and von Blankenburg, 2007)		
Common Pb correction	No common Pb correction		
Uncertainty	dates and Isotopic ratios are estimated at 2SD (standard deviation)		
References			
Horn and von Blankenburg, 2007, *Spectrochim. Acta* , Part B, **62**, 410–422.			

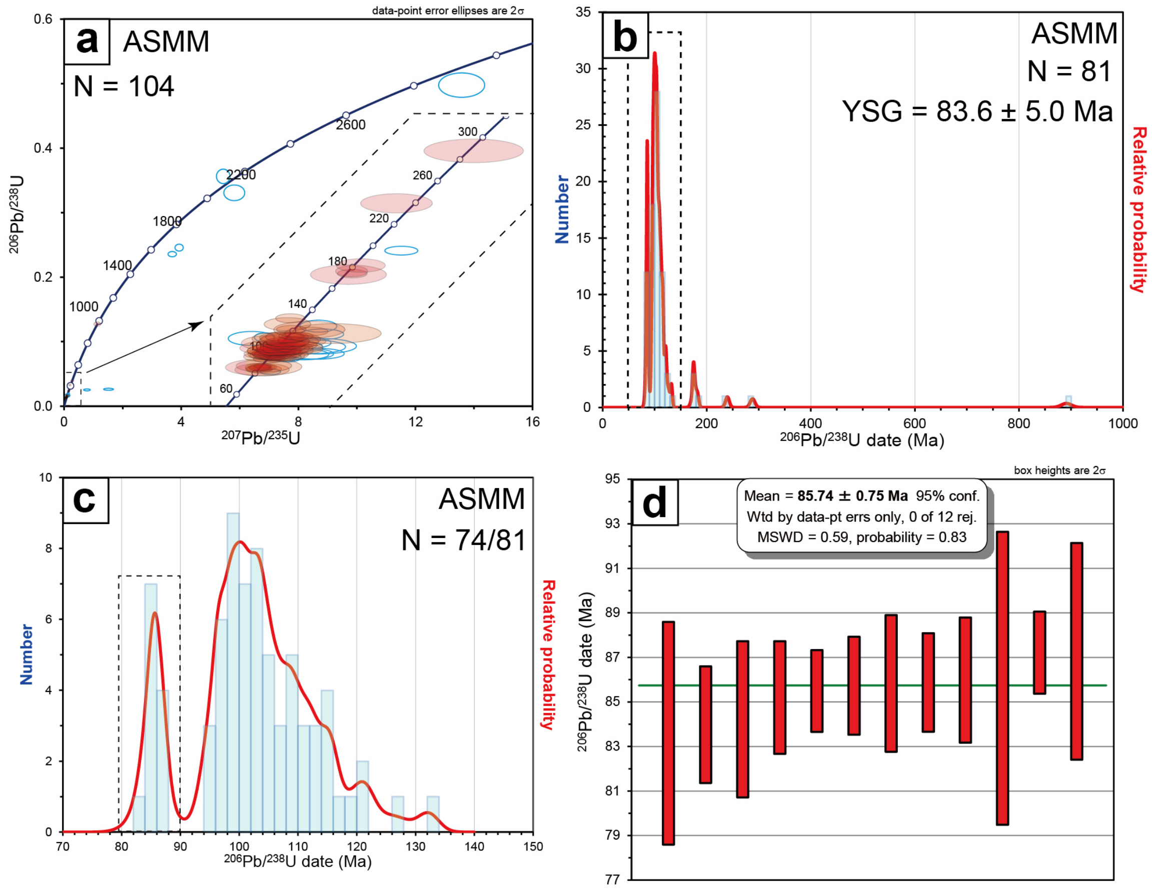

Fig. A1. U–Pb zircon data of the dated sample (ASMM). (a), The normal concordia plot (Gale and Mussett, 1973) of sample ASMM; (b), Relative probability density curve (RPDC) and histogram of all adopted data (bin width is 10 million year); (c), RPDC and histogram of younger data (<150 Ma; bin width is 2 million year); (d), Weighted mean $^{206}Pb/^{238}U$ date for the youngest cluster (ca. 87–84 Ma).